NATIONAL INSTITUTE OF AEROSPACE

Polar Crystallization of Boron Nitride Nanotube-Polyvinylidene Fluoride Nanocomposites

Dongwon Lee[a,b], Sang-Hyon Chu[b], Fuh-Gwo Yuan[a,b], Catharine Fay[c], and Cheol Park[c*]

[a]North Carolina State University, Department of Mechanical and Aerospace Engineering, Raleigh, NC, USA 27695; [b]National Institute of Aerospace, 100 Exploration Way, Hampton, VA, USA 23666; [c]NASA Langley Research Center, Advanced Materials and Processing Branch, Hampton, VA, USA 23681

12/04/2019

Outline

- **Introduction**
  Extreme Environments in Space Exploration
  Polyvinylidene Fluoride (PVDF) and difficulties in polar crystallization
  Multifunctional boron nitride nanotube (BNNT) as an inorganic nanofiller

- **Materials and characterizations**
  Fabrication of BNNT-PVDF composites
  FTIR[*1], XRD[*2], DSC[*3]
  d_{33}, piezoelectric coefficient

- **Summary and future plan**

FTIR[*1]: Fourier-transform infrared spectroscopy
XRD[*2]: X-ray diffraction
DSC[*3]: Differential scanning calorimetry

Extreme Environments in Space Exploration

NATIONAL INSTITUTE OF AEROSPACE

The lightweight and robust sensing & actuating materials are required in harsh environment.

- Harsh thermal cycle of -175 ~ 160 ℃
- High UV/radiation exposure
- Hypervelocity (3 km/s) impact of micrometeorite and orbital debris (MMOD)

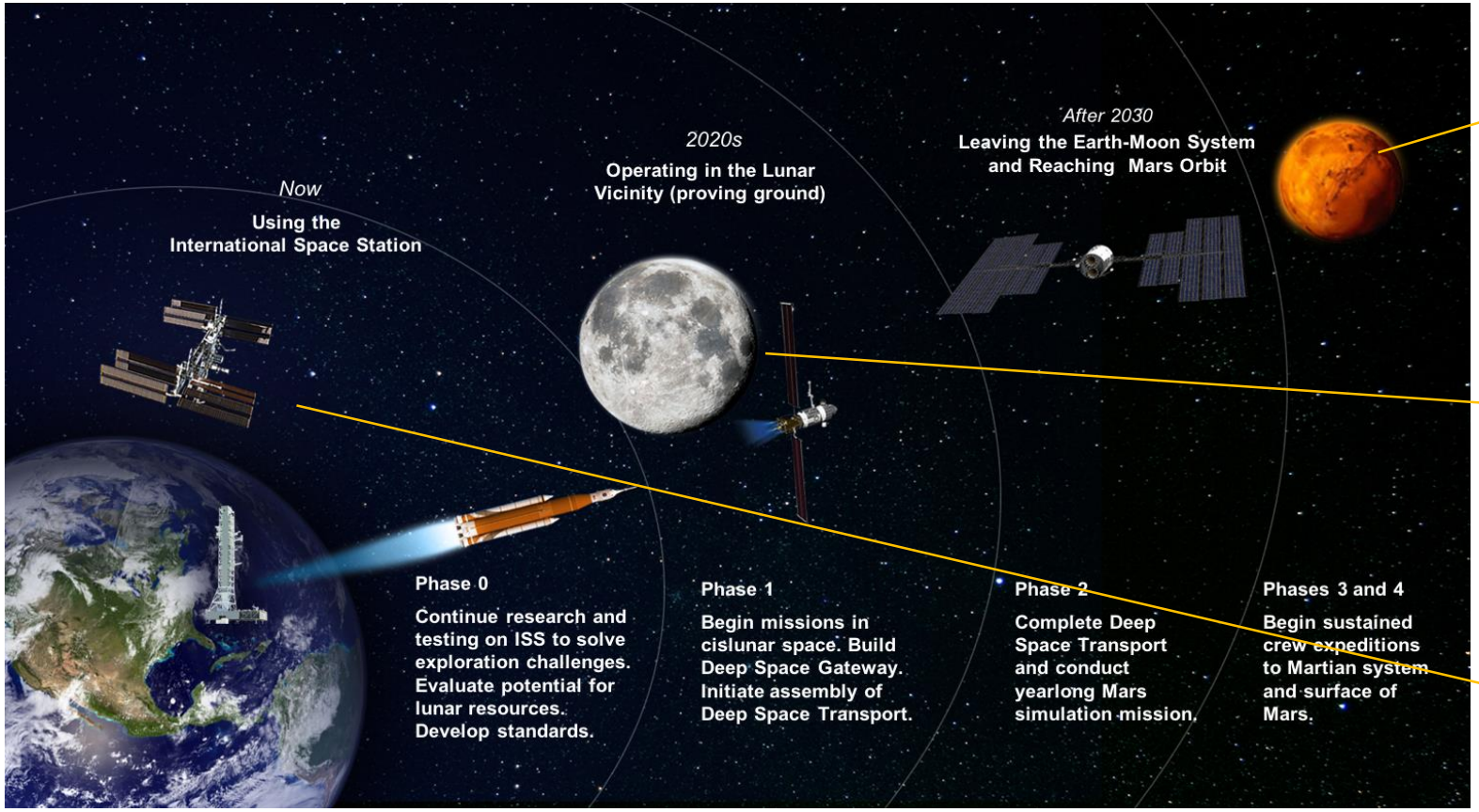

NASA deep space exploration roadmap

Mars surface
-126 to 21˚C
Sand storm
Radiation
Entry, Descent, & Landing

Lunar surface
-173 to 127˚C
-247˚C (25K) at pole
< 10^{-12} torr
Deep & Vacuum UV
Sharp abrasive edge dust
Radiation

International Space Station
-175 to 160˚C
10^{-6} to 10^{-9} torr
UV/AO, GCR/SPE/Van Allen Belt
MMOD
Microgravity

All images credit: NASA

Polyvinylidene fluoride (PVDF)

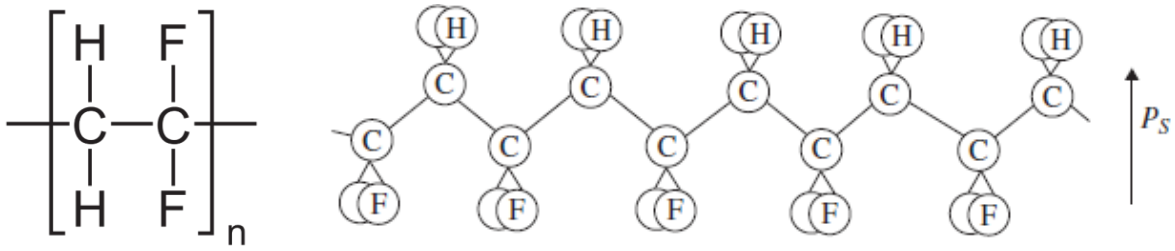

Schematic chemical structure of PVDF (β phase)

Features

- Act as both sensor and actuator (piezoelectricity)
- Flexible and durable (robust)
- Lightweight
- Easy & inexpensive fabrication
- Biocompatible
- Low mechanical impedance

Table 1. Properties of PVDF and PZT-5A

Property	Symbol	PVDF	PZT-5A
Elastic modulus (Pa)	Y	2×10^9	7.4×10^{10}
Poisson's ratio	ν	0.34	0.35
Relative dielectric permittivity	ε_r	12	1800
Piezoelectric strain coefficient (pC/N)	d_{31}	22	-175
	d_{33}	-30	450
Piezoelectric stress coefficient (Vm/N)	g_{31}	0.216	-0.011
	g_{33}	-0.33	0.027
Electromechanical coupling coefficient	k_{31}	0.14	0.34

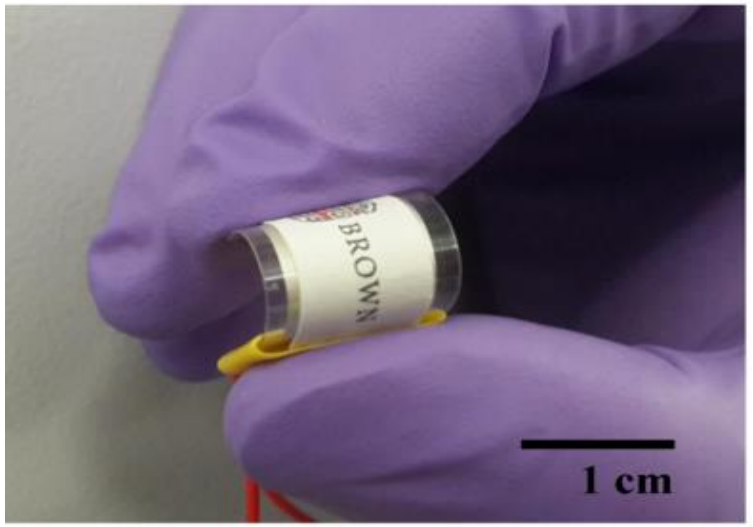

Flexibility of fluoropolymer

Kumar et al., *Smart Polymer Nanocomposites* (2017) [1]

Won et al., *Applied Physics Letters* (2015) [2]

Challenges in β phase transformation of PVDF

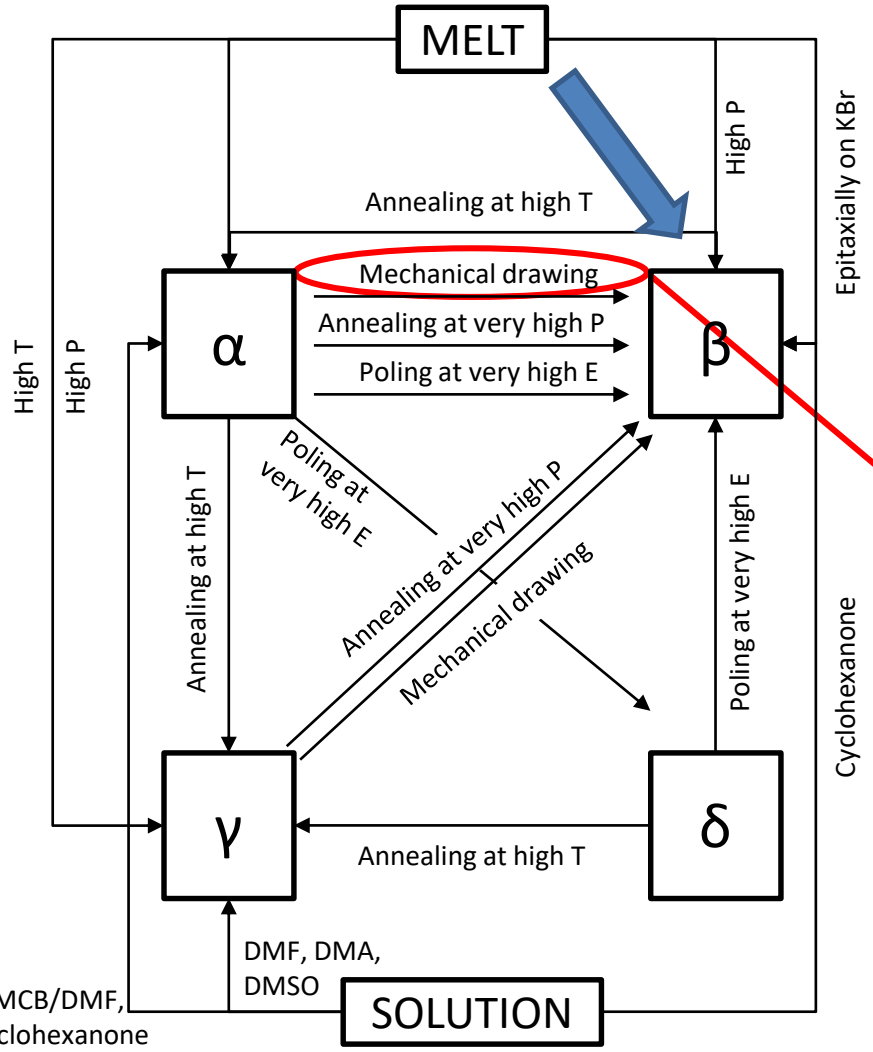

Overview of phase transformations of PVDF

Bassett et al., *Developments in crystalline polymers* (1982) [3]

Li et al., *RSC Advances* (2014) [4]

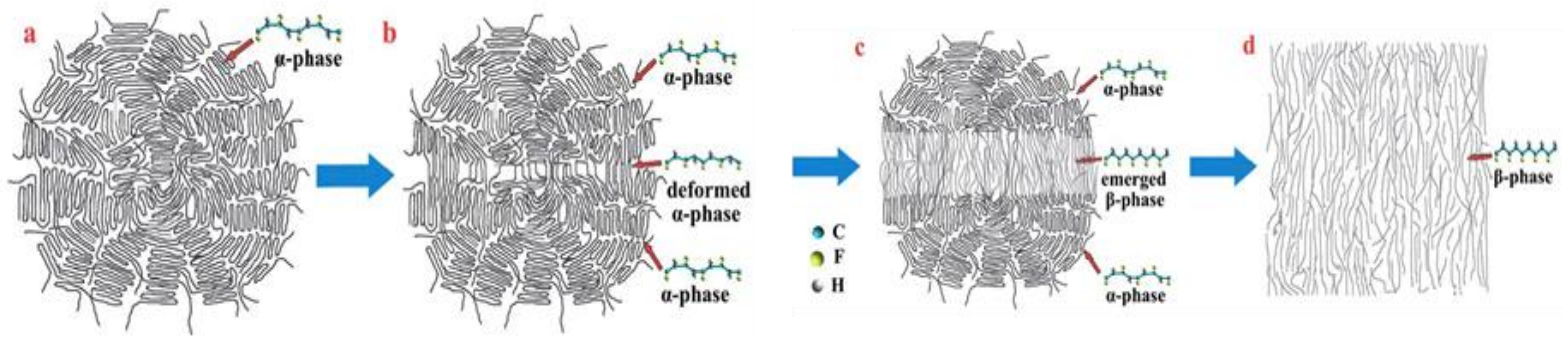

The transformation process from α-crystal to β-crystal of PVDF by mechanical stretching

Mechanical drawing (α → β)
: The most effective method

Limitations of mechanical drawing

a. **Low crystallinity**:
low electromechanical coupling coefficient

b. **Defect**:
easy depolarization

c. **Limited shape**:
film type only

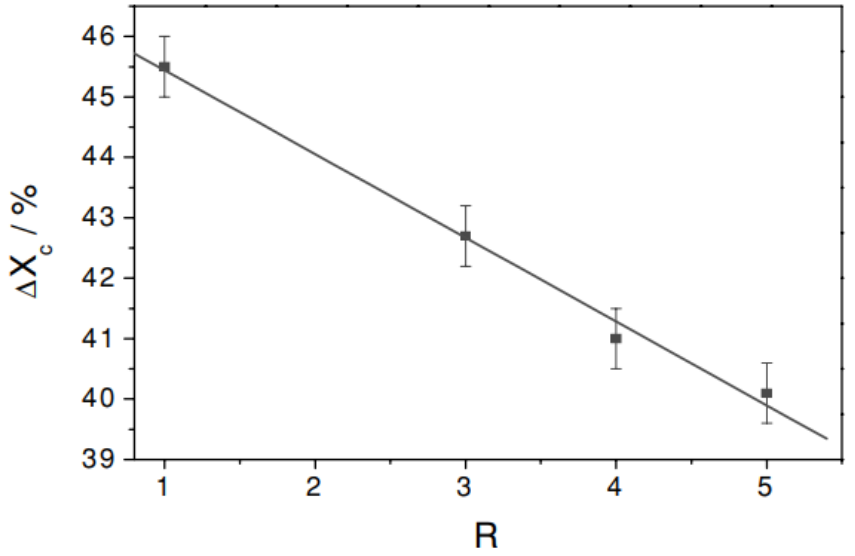

Degree of crystallinity ΔXc with increasing stretch ratio (R)

Sencadas et al., *Journal of Macromolecular Science®* (2009) [5]

Boron nitride nanotube (BNNT)

- Structural analog to CNTs containing hexagonal BN with tubular morphology
- High tensile strength (~30 GPa)
- High elastic modulus (~1.2 TPa)
- High thermal conductivity (>500 W/mK)
- Piezoelectricity (Larger than PVDF predicted)
- High thermal stability (800~900 °C in air)
- Good electrical insulation (Wide bandgap 5.5~6.0 eV)
- Super-hydrophobic, biocompatible…

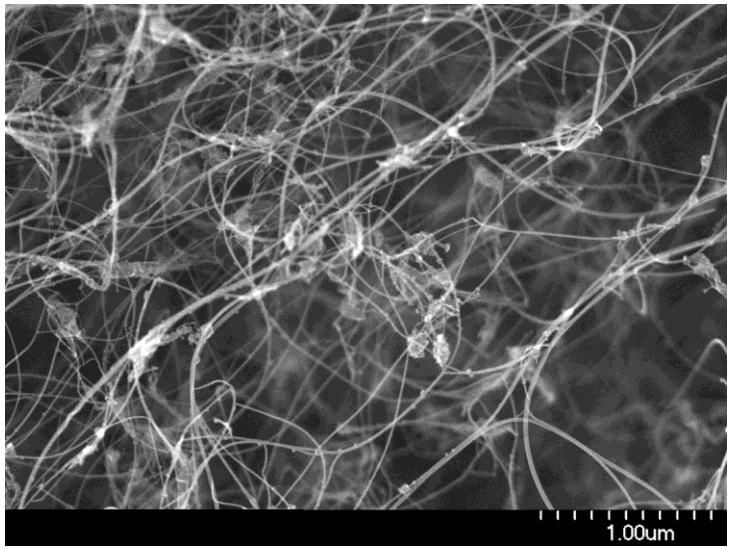

Scanning electron microscope image of boron nitride nanotube as received from BNNT, LLC

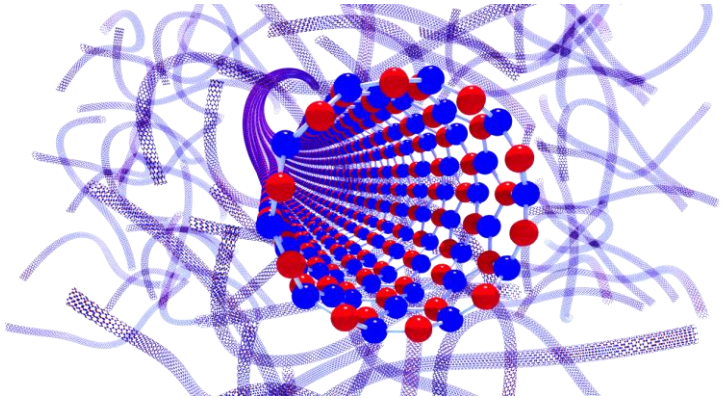

Schematic drawing of boron nitride nanotube

Images credit: NASA

Lee et al., *Micro-and Nanotechnology Sensors, Systems, and Applications XI* (2019) [6]

Applications of BNNTs

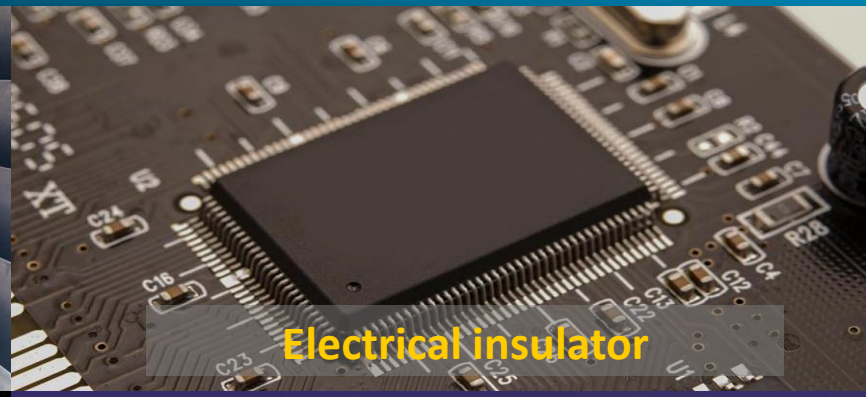

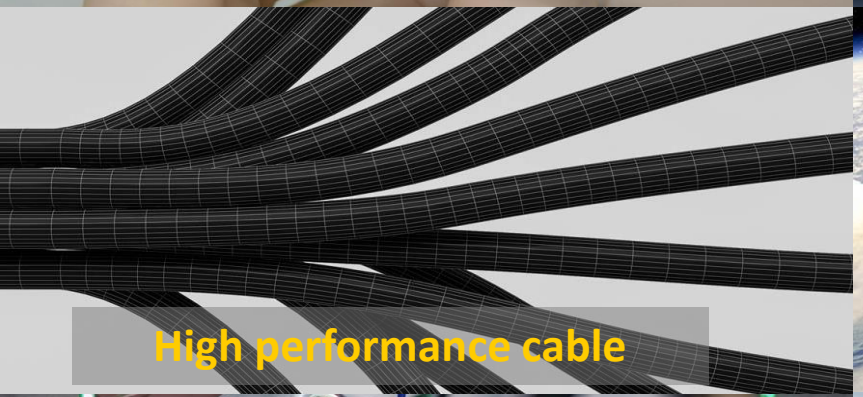

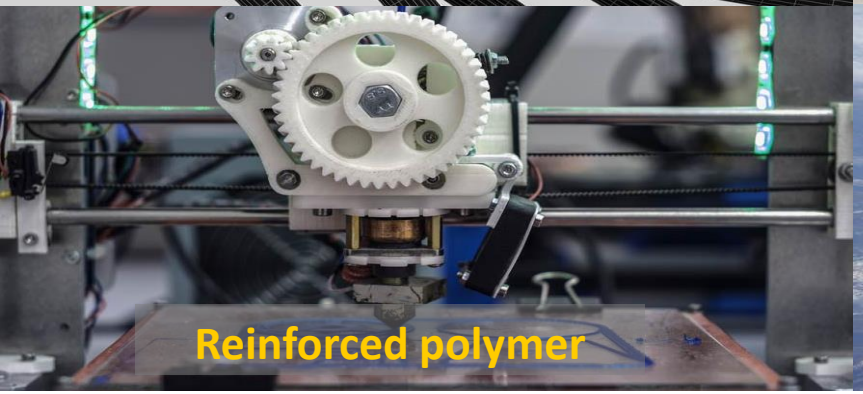

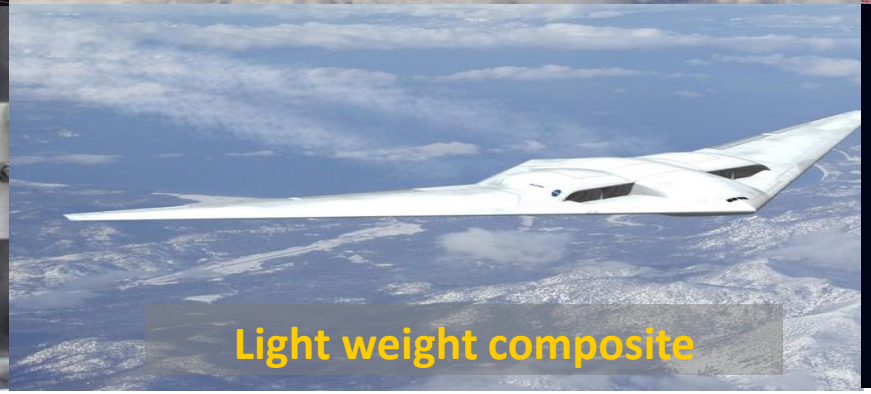

Applications of boron nitride nanotubes (BNNTs)

All images credit: BNNT. LLC and NASA

Fabrication of BNNT-PVDF composites

PVDF

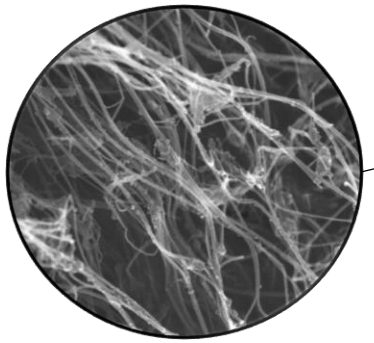

BNNT

Dimethylacetamide (DMAc)

Transfer

Dry in vacuum, at 60C overnight

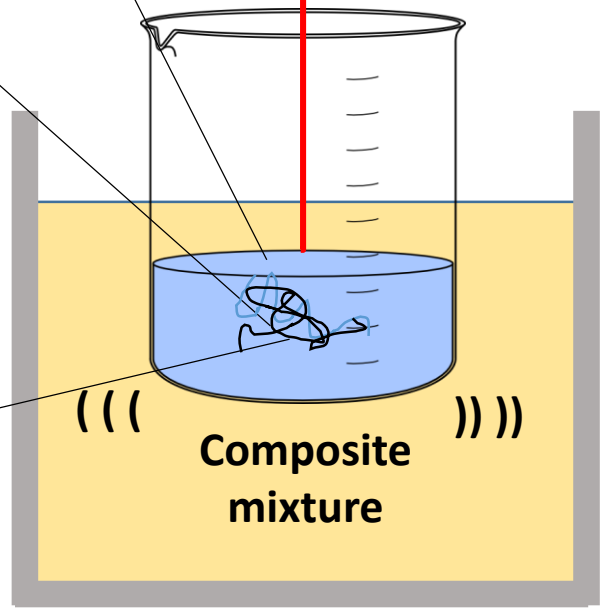

Cup horn sonicator (48W, 10min)

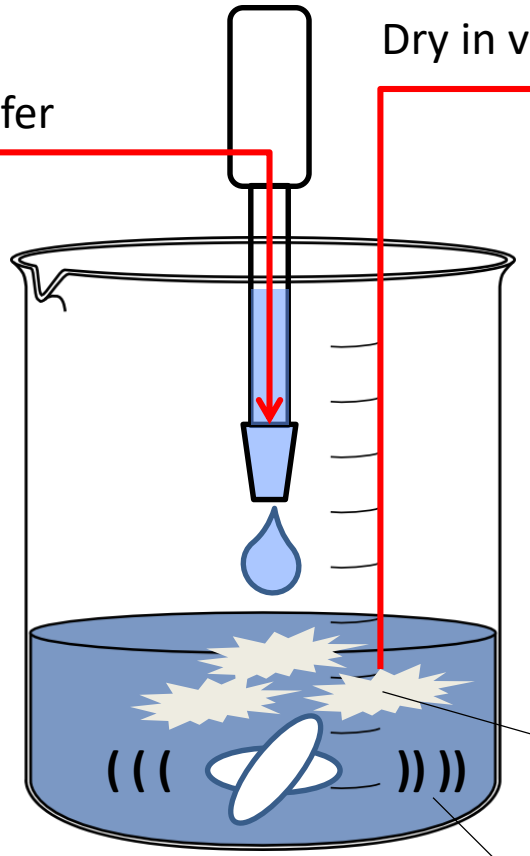

Coagulation bath with a stirring bar

Deionized water (DI H_2O)

BNNT-PVDF composite

Hot press

Schematic procedure of fabricating BNNT-PVDF nanocomposite

SEM images of hot pressed BNNT-PVDF composites

NATIONAL INSTITUTE OF AEROSPACE

(a) 0% BNNT-PVDF

(b) 5% BNNT-PVDF

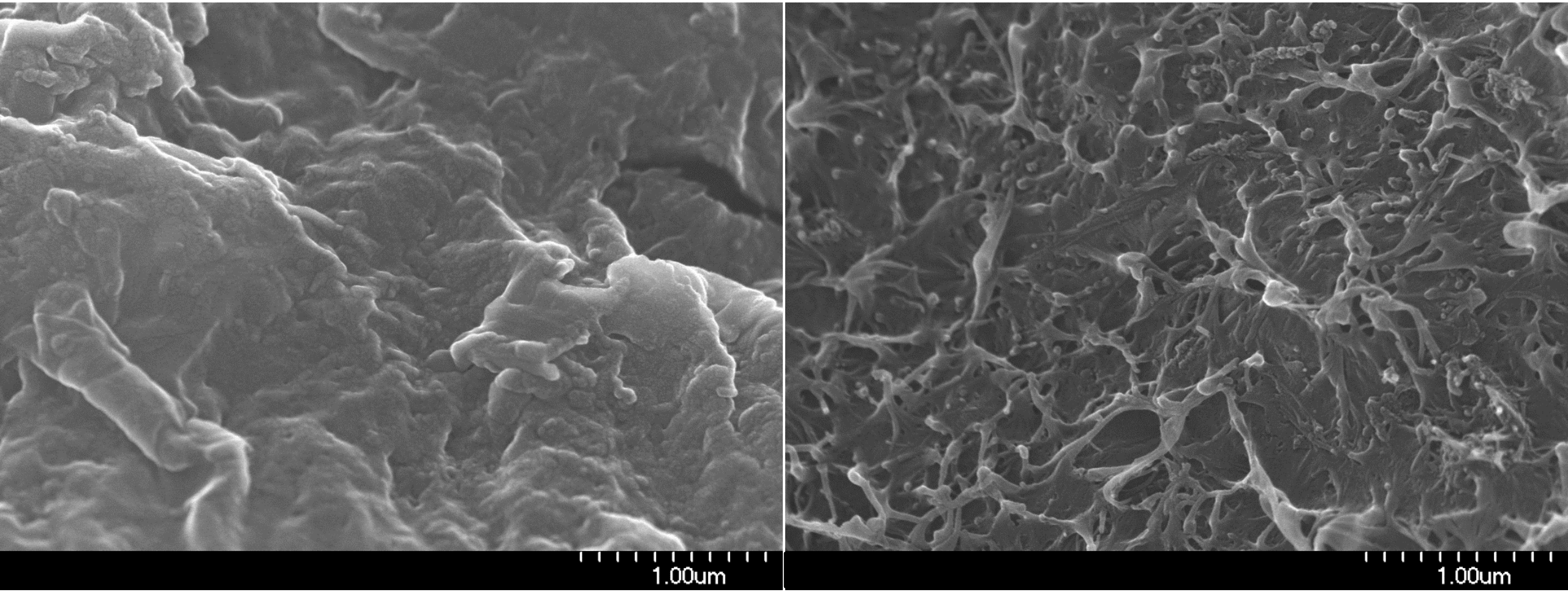

Scanning electron microscope images of liquid nitrogen-cut BNNT-PVDF composites. (a) pristine PVDF, (b) 5% BNNT-PVDF

FTIR analysis of hot-pressed BNNT-PVDF composites

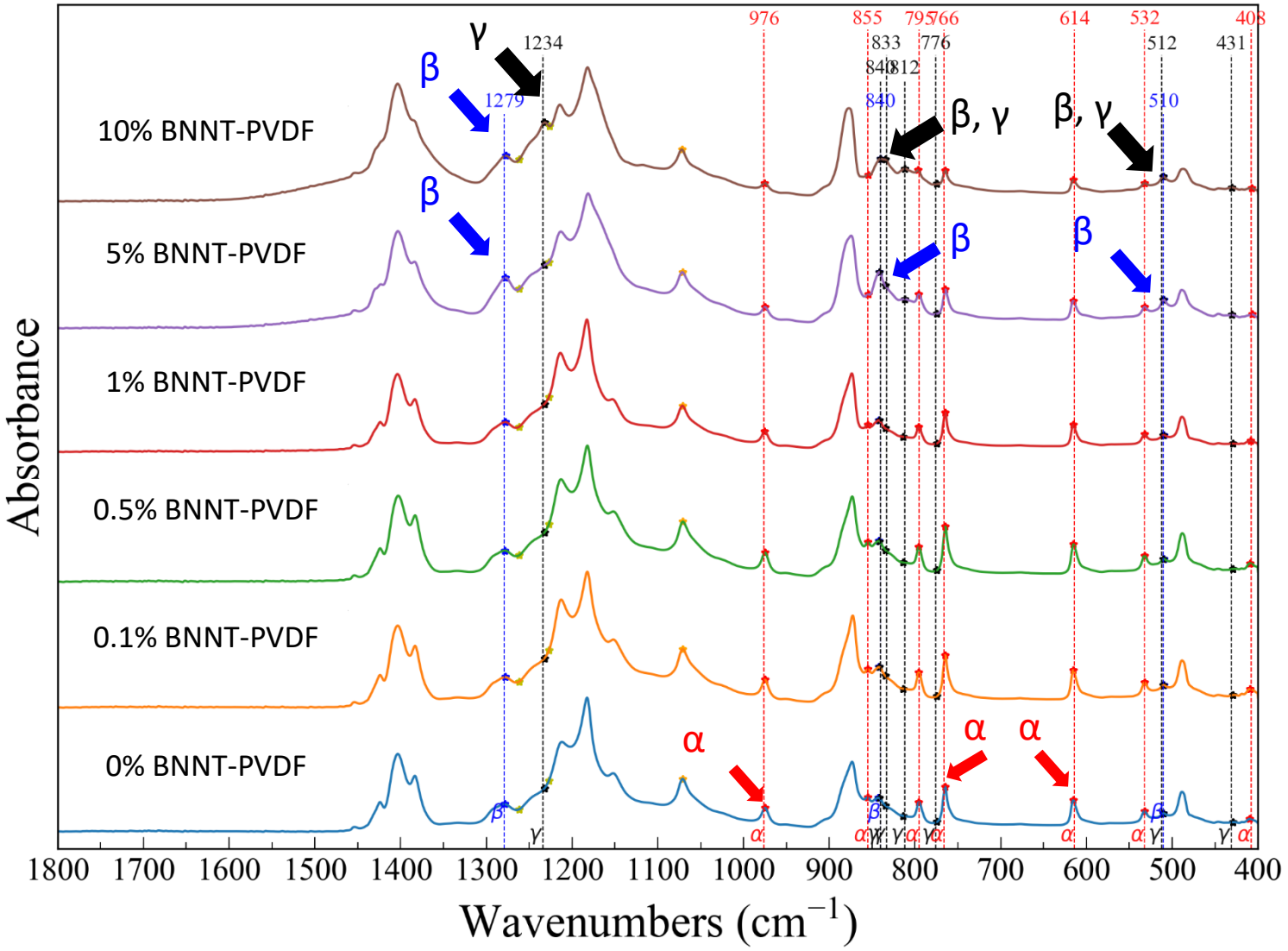

FTIR absorbance peaks of hot-pressed BNNT-PVDF composites

44% of the β fraction was determined in 5 wt% BNNT-PVDF after the hot pressing at 171 C.

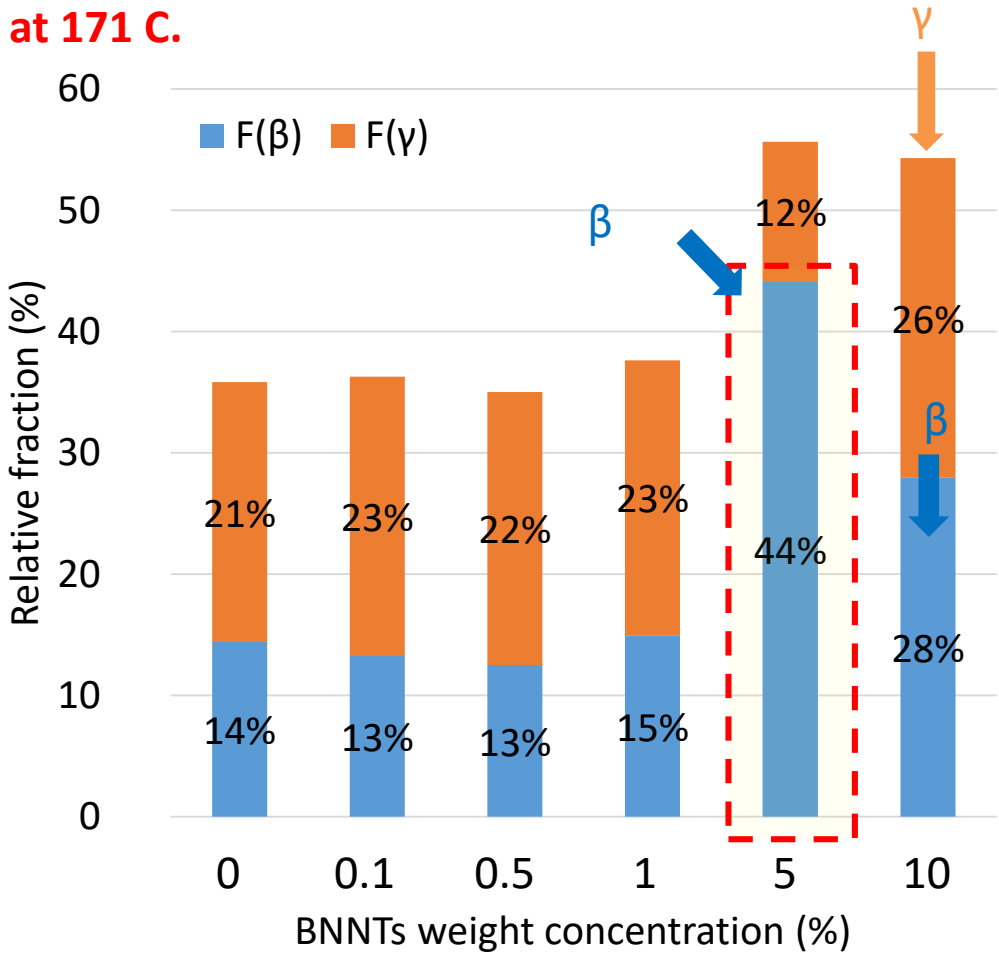

Polar fractions (%) of hot-pressed BNNT-PVDF composites

XRD analysis of hot-pressed BNNT-PVDF composites

BNNTs increased β crystal peak at 2θ = 20.8 ° in XRD analysis.

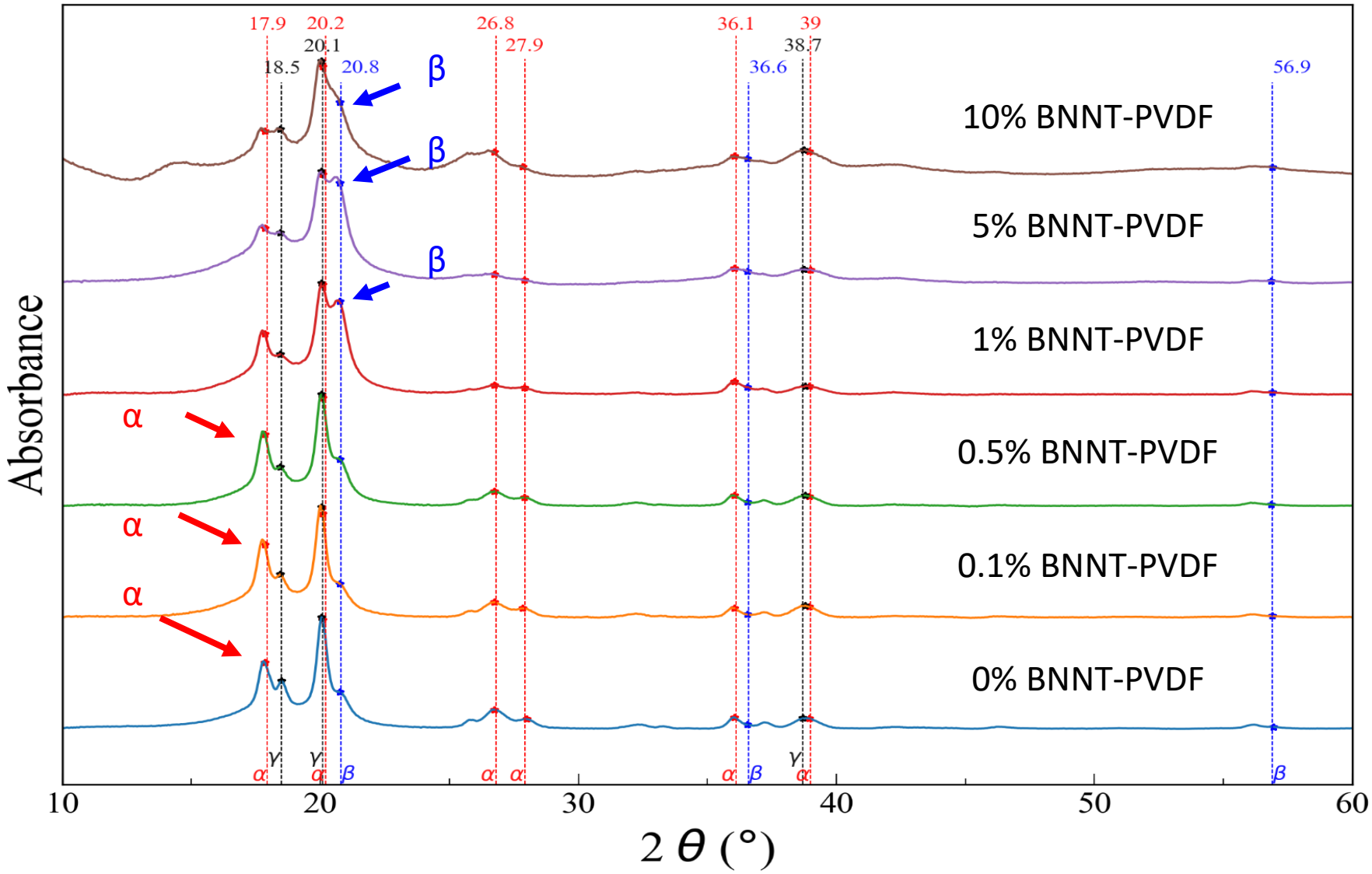

Wide-angle X-ray diffraction peaks of hot-pressed BNNT-PVDF composites

DSC analysis of hot-pressed BNNT-PVDF composites

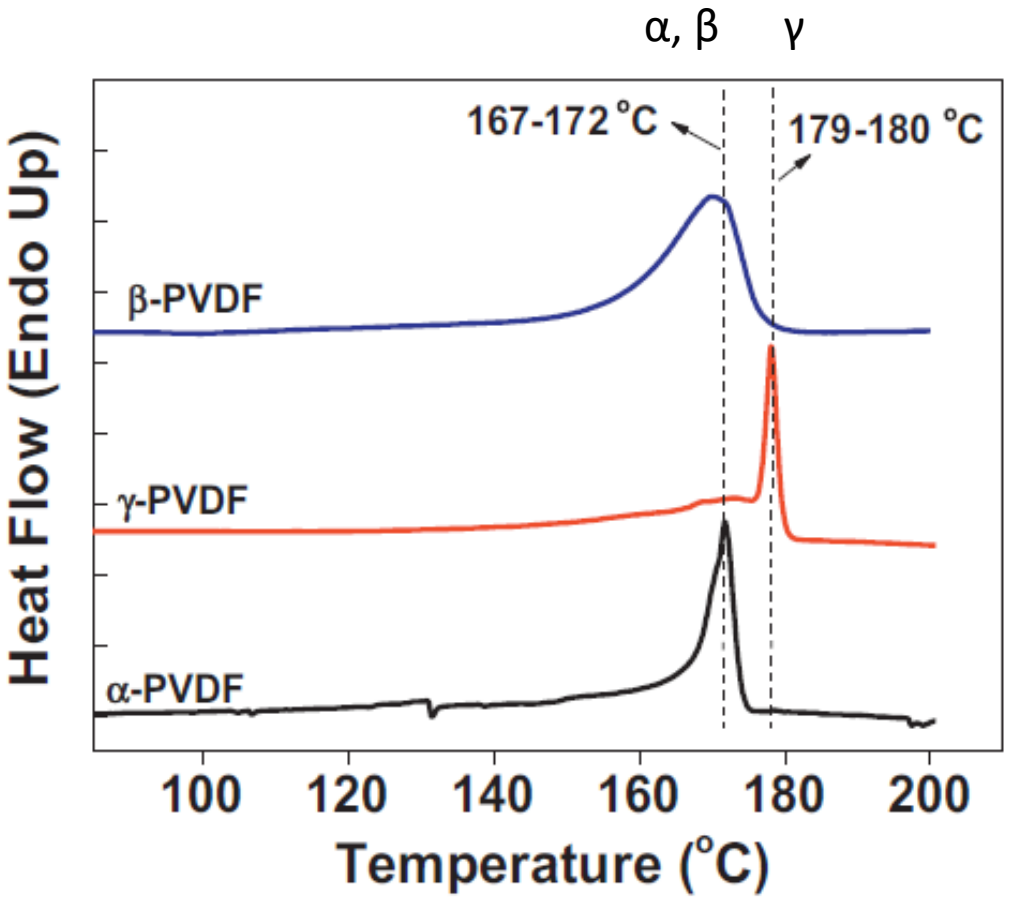

Melting peak of PVDF polymorphs (β,γ, α)

Martins et.al., *Progress in polymer science* (2014) [7]

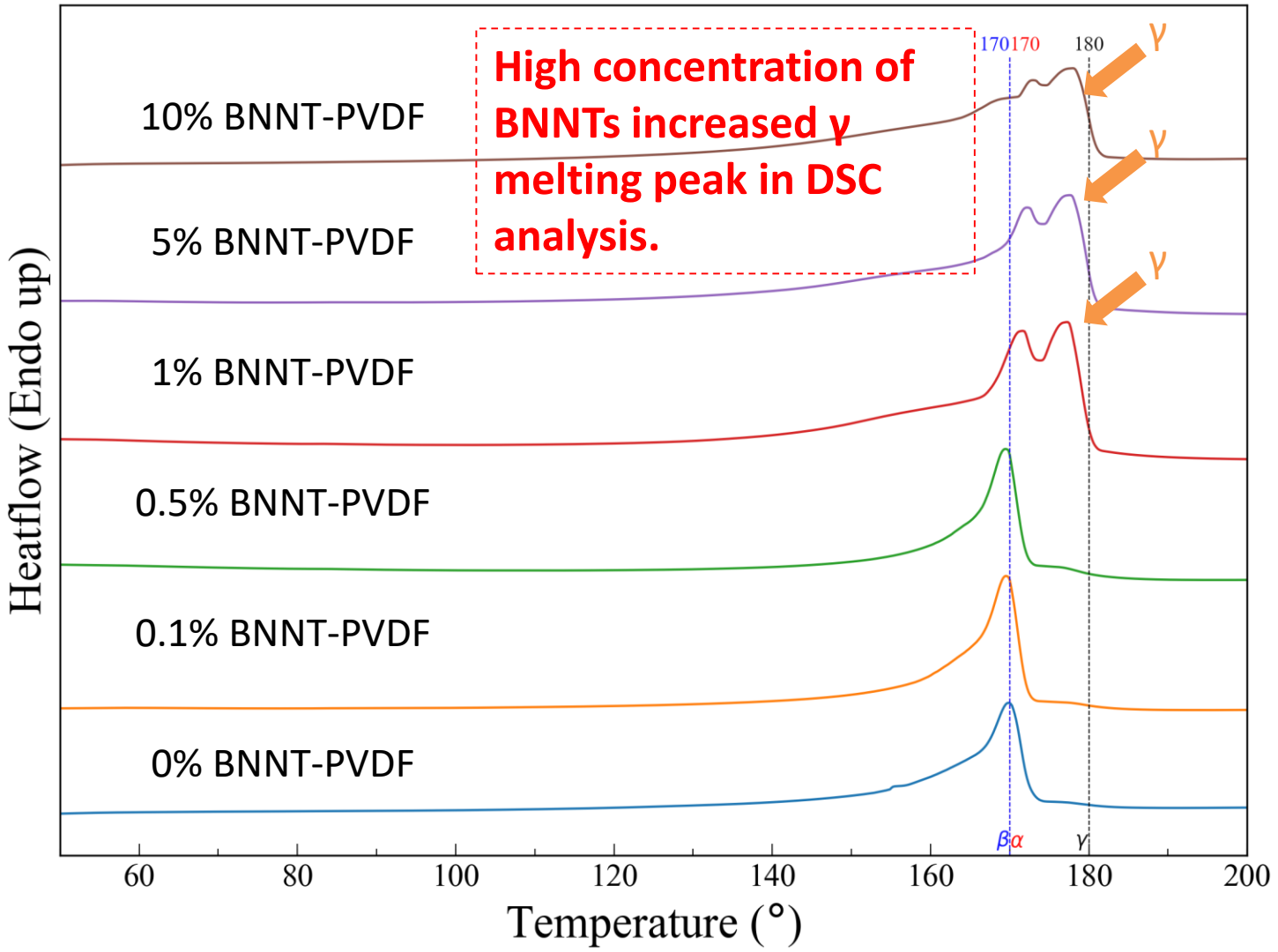

Melting peak of hot-pressed BNNT-PVDF composites

FTIR analysis of recrystallization of BNNT-PVDF composites

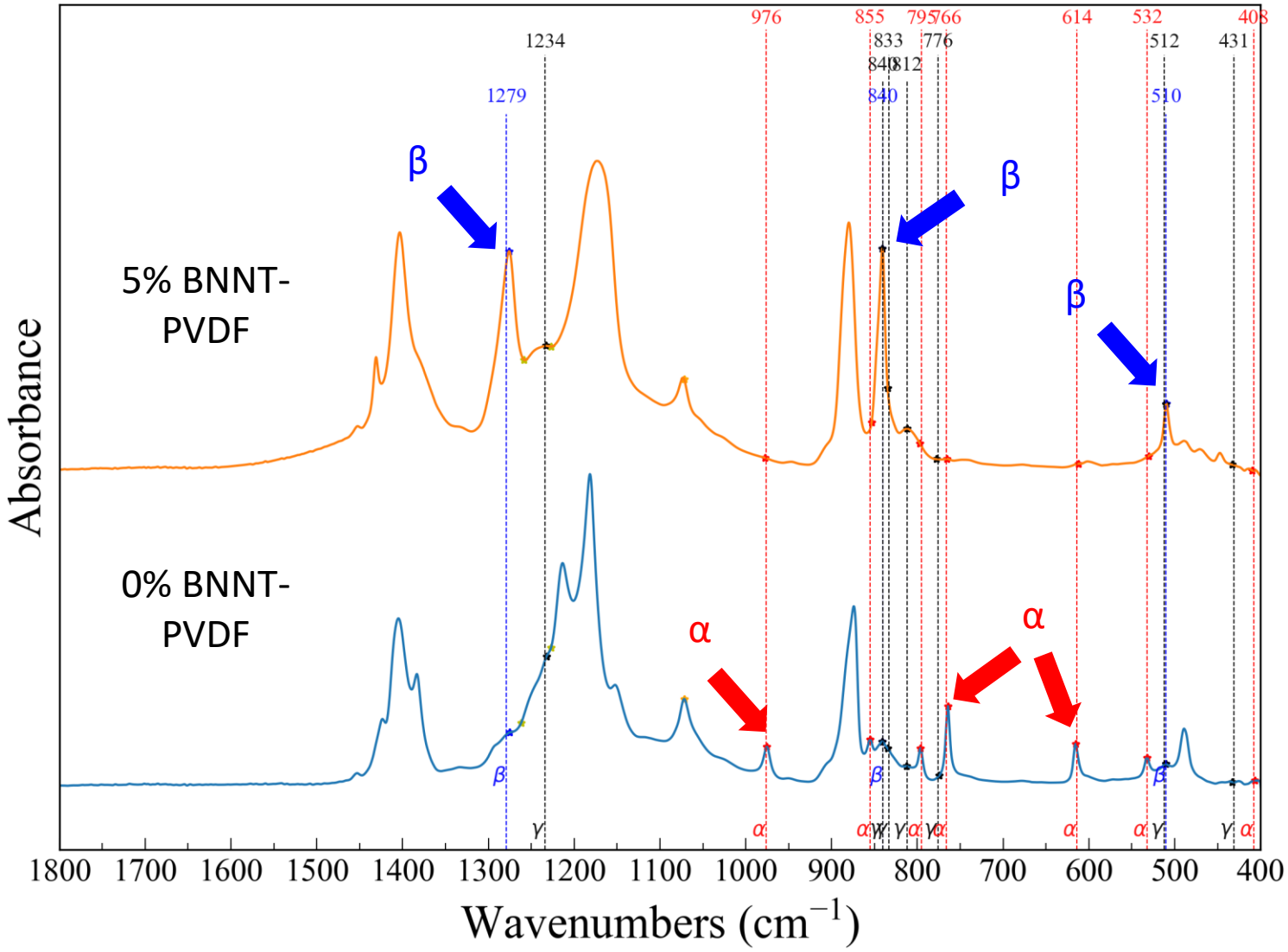

FTIR absorbance peaks of melt recrystallized BNNT-PVDF composites

Incorporation of **5 wt% BNNTs** in PVDF matrix dramatically increased the mole fraction of **β** up to **92%** after recrystallization from the melt, **without mechanical stretching!**

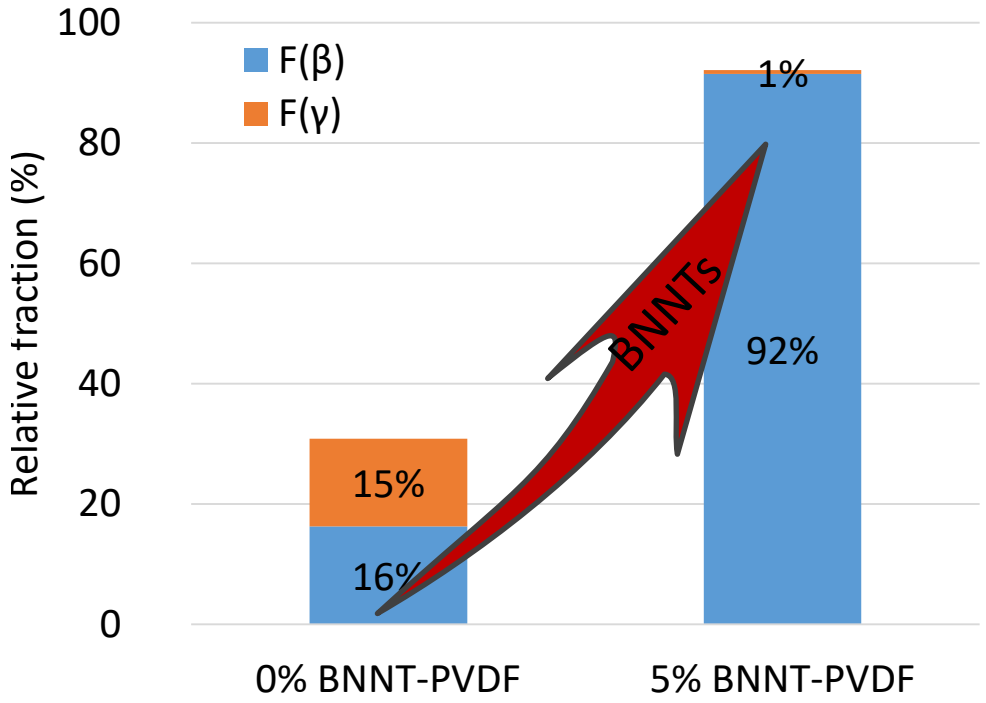

Polar mole fractions (%) of re-crystallized BNNT-PVDF composites based on the peak-valley method

XRD analysis of melt recrystallized BNNT-PVDF composites

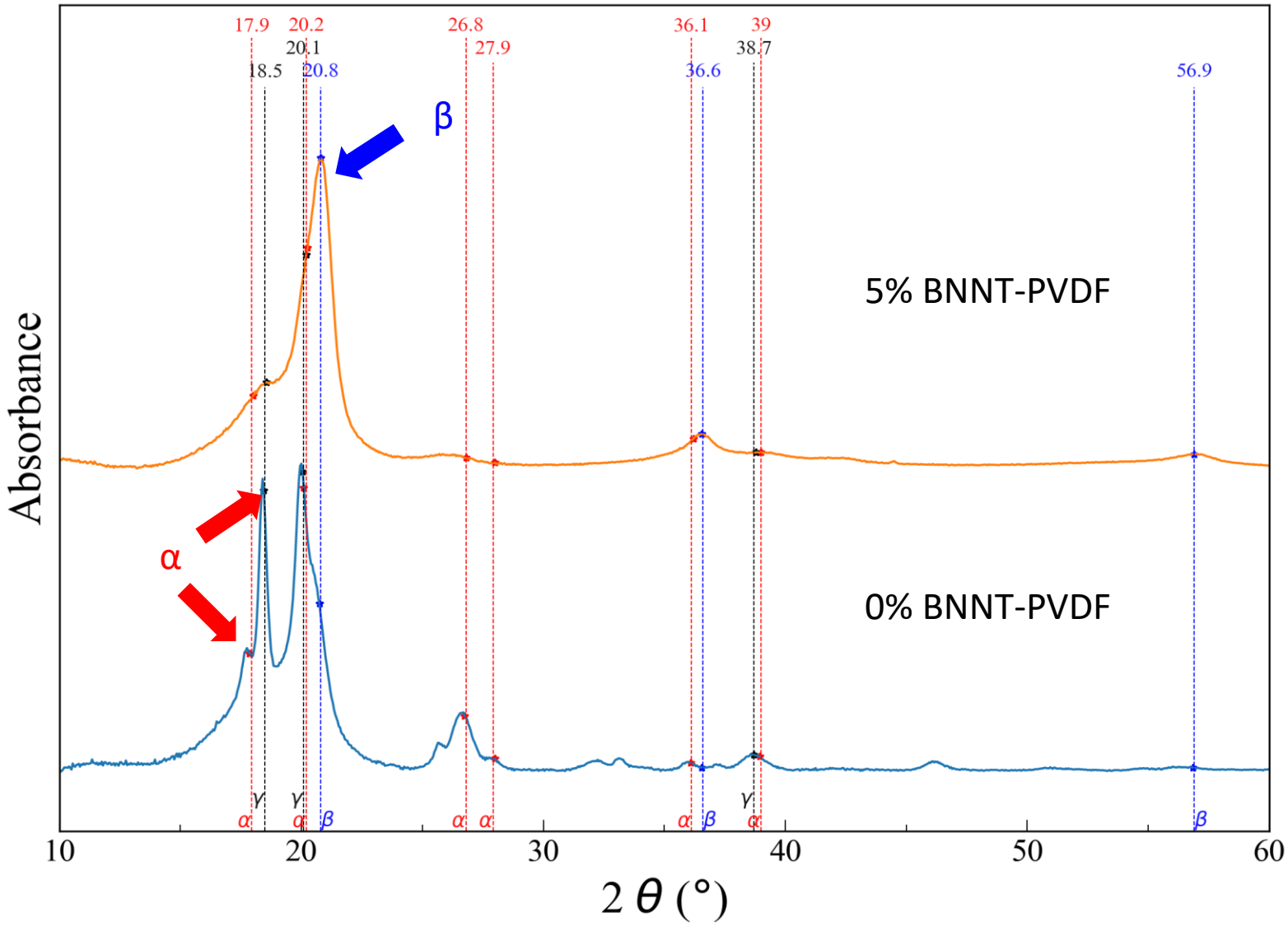

Wide-angle X-ray diffraction peaks of melt recrystallized BNNT-PVDF composites

Incorporation of **5 wt% BNNT** in PVDF matrix dramatically increased **β peak at 20.8 °** in XRD analysis.
It is a good alignment with FTIR results.

d_{33}, piezoelectric coefficient

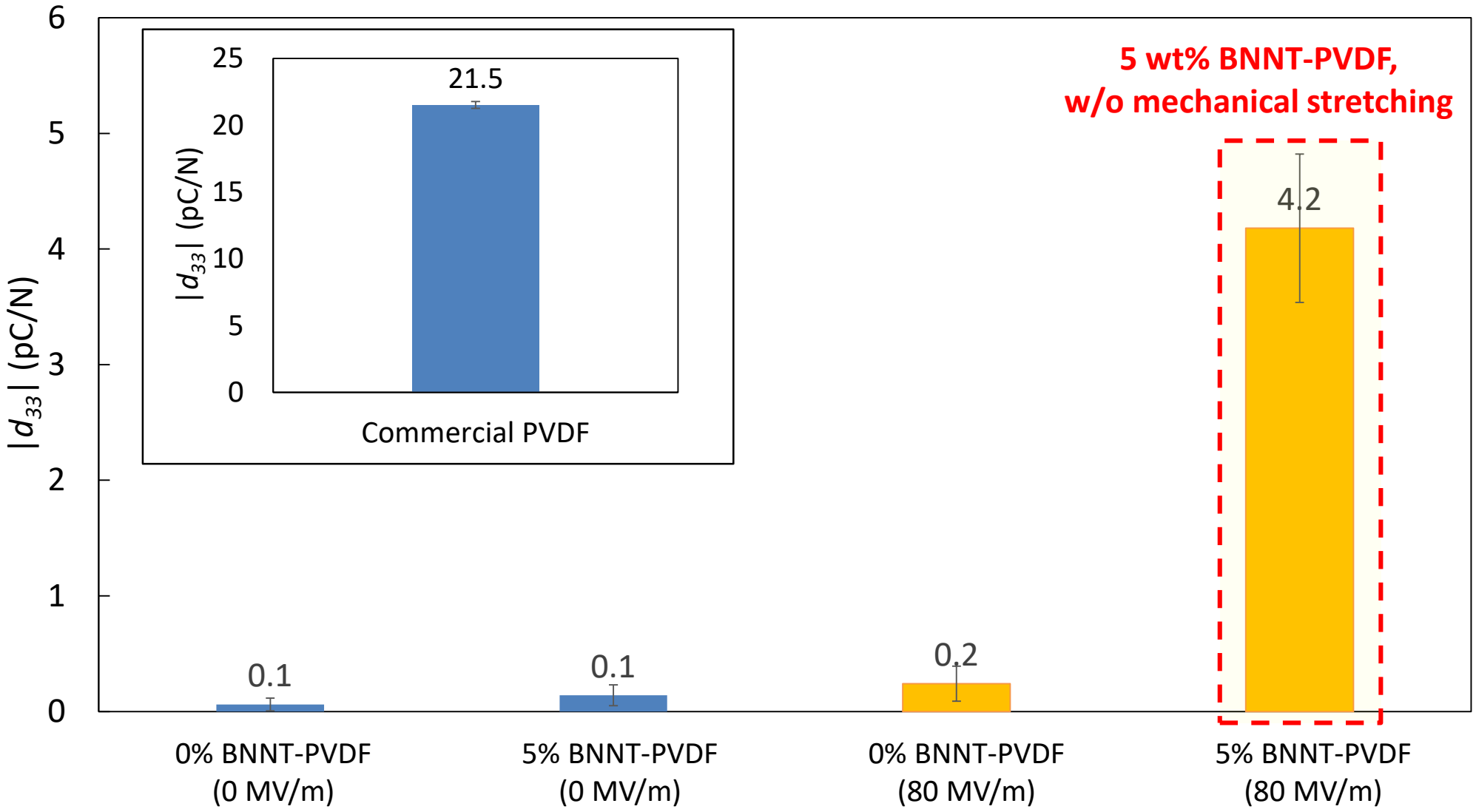

Piezoelectric coefficient, d_{33} measured by a d_{33} meter (direct piezoelectric method)

Tensile test of hot-pressed BNNT-PVDF composites

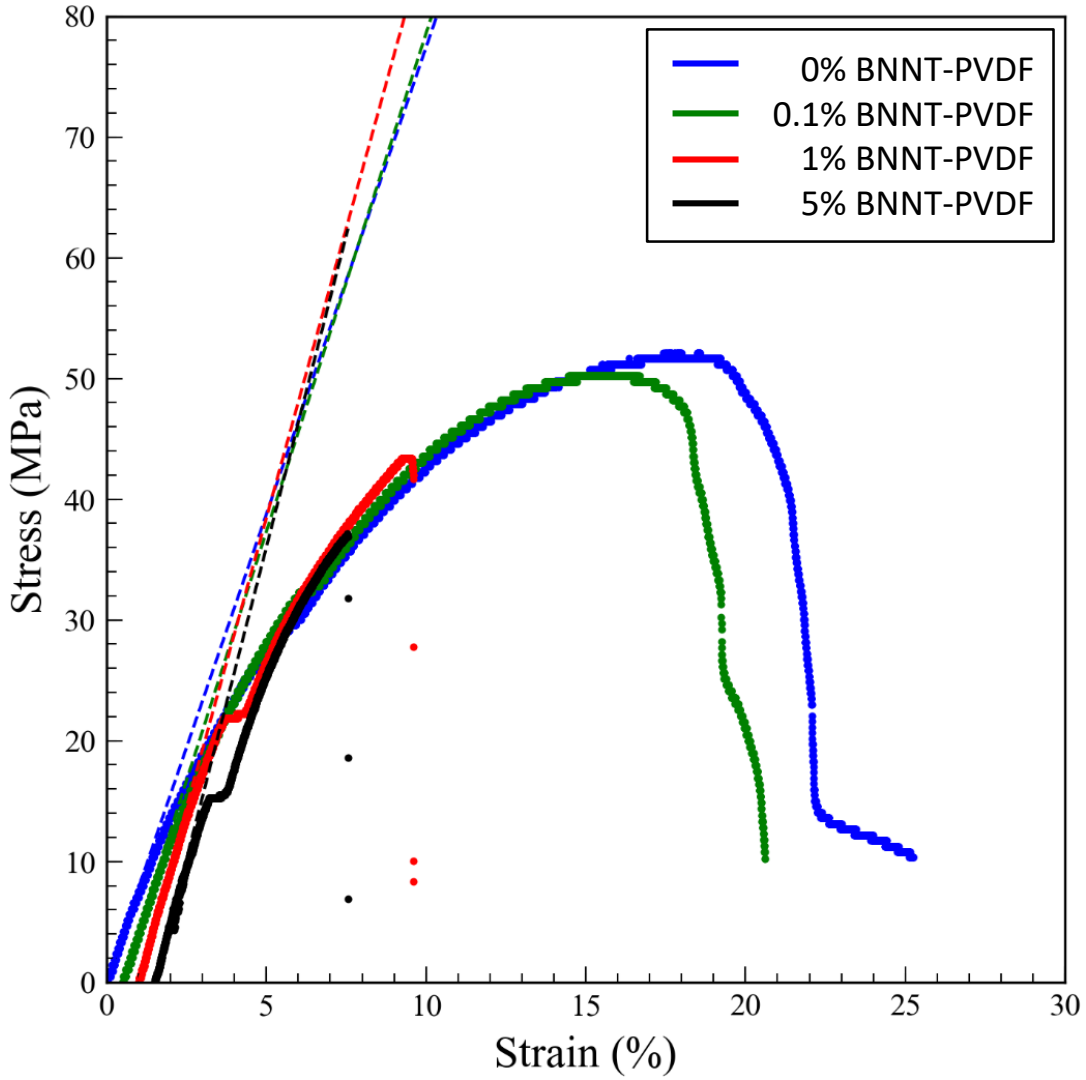

Stress-strain curve of hot-pressed BNNT-PVDF composites

"33% increase of elastic modulus of was observed in 5 wt% BNNT-PVDF"

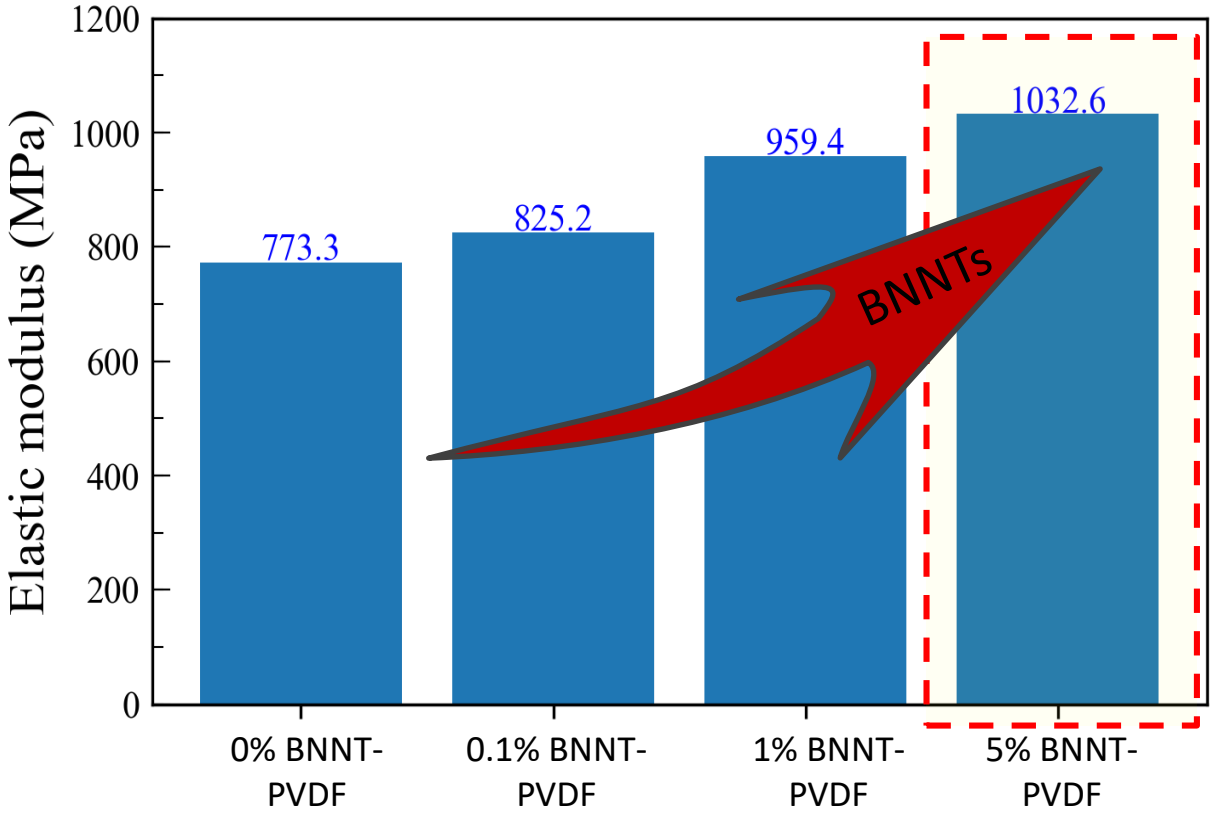

Elastic modulus of hot-pressed BNNT-PVDF composites

Summary and future plan

- Incorporation of 5 wt% BNNTs as a nucleating agent induced up to 92% β conformation of PVDF from the melt, without mechanical stretch.
- The piezoelectric coefficient, $|d_{33}|$ = 4.2 pC/N was measured by a commercial d_{33} meter in 5 wt% BNNT-PVDF composite while 0 wt% BNNT-PVDF did not show the piezoelectric behavior.
- Incorporation of 5 wt% of BNNTs improved 33% of elastic modulus of the pristine PVDF matrix.
- Mechanism study of the β crystallization of BNNT-PVDF from the melt and their thermal behavior study are on the way.

Acknowledgement

Financial support provided by the Graduate Research Assistantship (GRA) from National Institute of Aerospace(NIA) through Air Force Office of Scientific Research (AFOSR), Korea Institute of Science and Technology (KIST). Facilities at NASA Langley Center were utilized through space act agreements.

References

[1] Kumar, Aravind, Shaikh Faruque Ali, and A. Arockiarajan. "Energy Harvesting from Crystalline and Conductive Polymer Composites." *Smart Polymer Nanocomposites*. Springer International Publishing, 2017. 43-75.

[2] Won, Sung Sik, et al. "Piezoelectric poly (vinylidene fluoride trifluoroethylene) thin film-based power generators using paper substrates for wearable device applications." *Applied Physics Letters* 107.20 (2015): 202901.

[3] Bassett, David Clifford, ed. *Developments in crystalline polymers*. Vol. 1. London: Applied Science Publishers, 1982.

[4] Li, Li, et al. "Studies on the transformation process of PVDF from α to β phase by stretching." *RSC Advances* 4.8 (2014): 3938-3943

[5] Sencadas, Vitor, Rb Gregorio Jr, and Senentxu Lanceros-Méndez. "α to β phase transformation and microestructural changes of PVDF films induced by uniaxial stretch." *Journal of Macromolecular Science®* 48.3 (2009): 514-525.

[6] Lee, Dongwon, et al. "Piezoelectric characterization of boron nitride nanotube-polyurethane composites." *Micro-and Nanotechnology Sensors, Systems, and Applications XI*. Vol. 10982. International Society for Optics and Photonics, 2019.

[7] Martins, P., A. C. Lopes, and S. Lanceros-Mendez. "Electroactive phases of poly (vinylidene fluoride): Determination, processing and applications." *Progress in polymer science* 39.4 (2014): 683-706.

Backup Information

Polymorphs of PVDF

Favored piezoelectric phase

α conformation (TGTG')

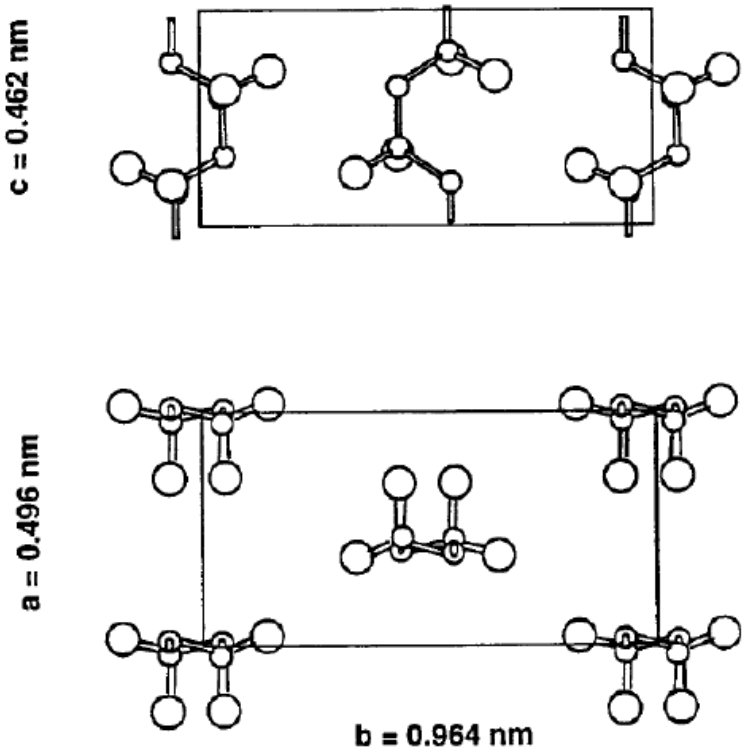

β conformation (TT)

(Dipole: 8×10^{-30} C m)

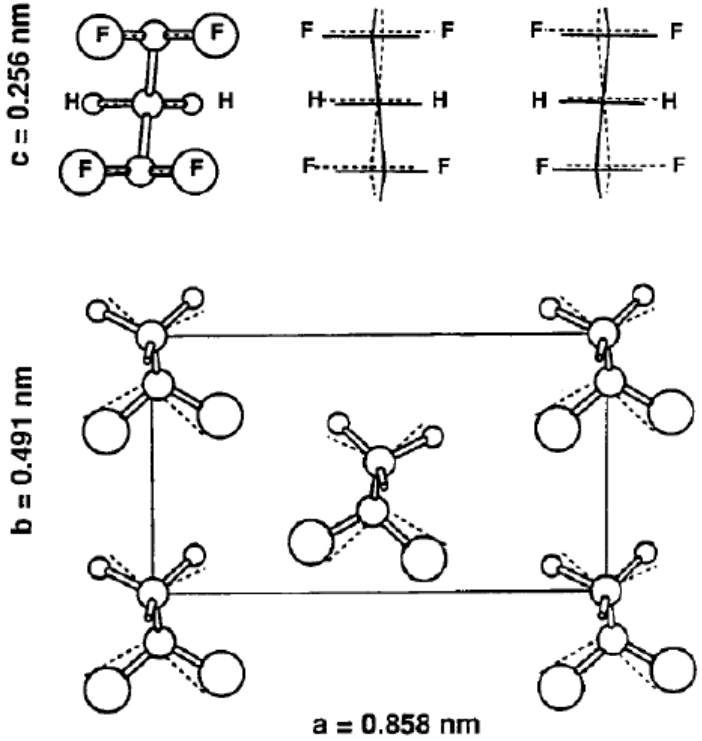

γ conformation (TTTGTTTG')

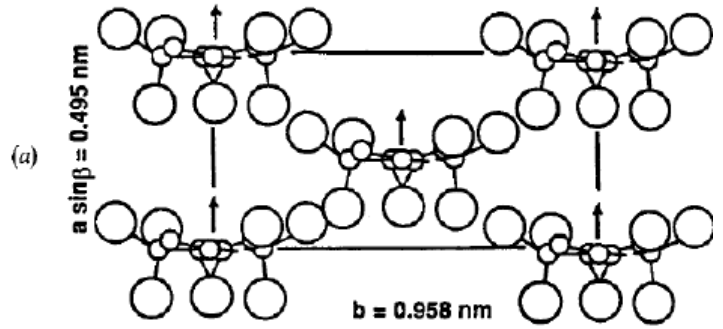

Delta conformation (TGTG')

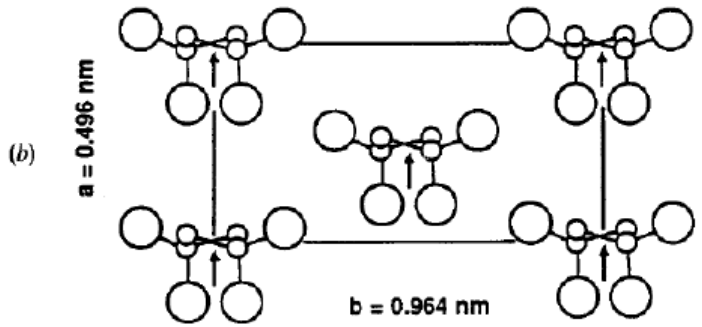

Omar, Abid., *Autex: Institut fur Textiltechnik* (2008)

Degree of crystallinity

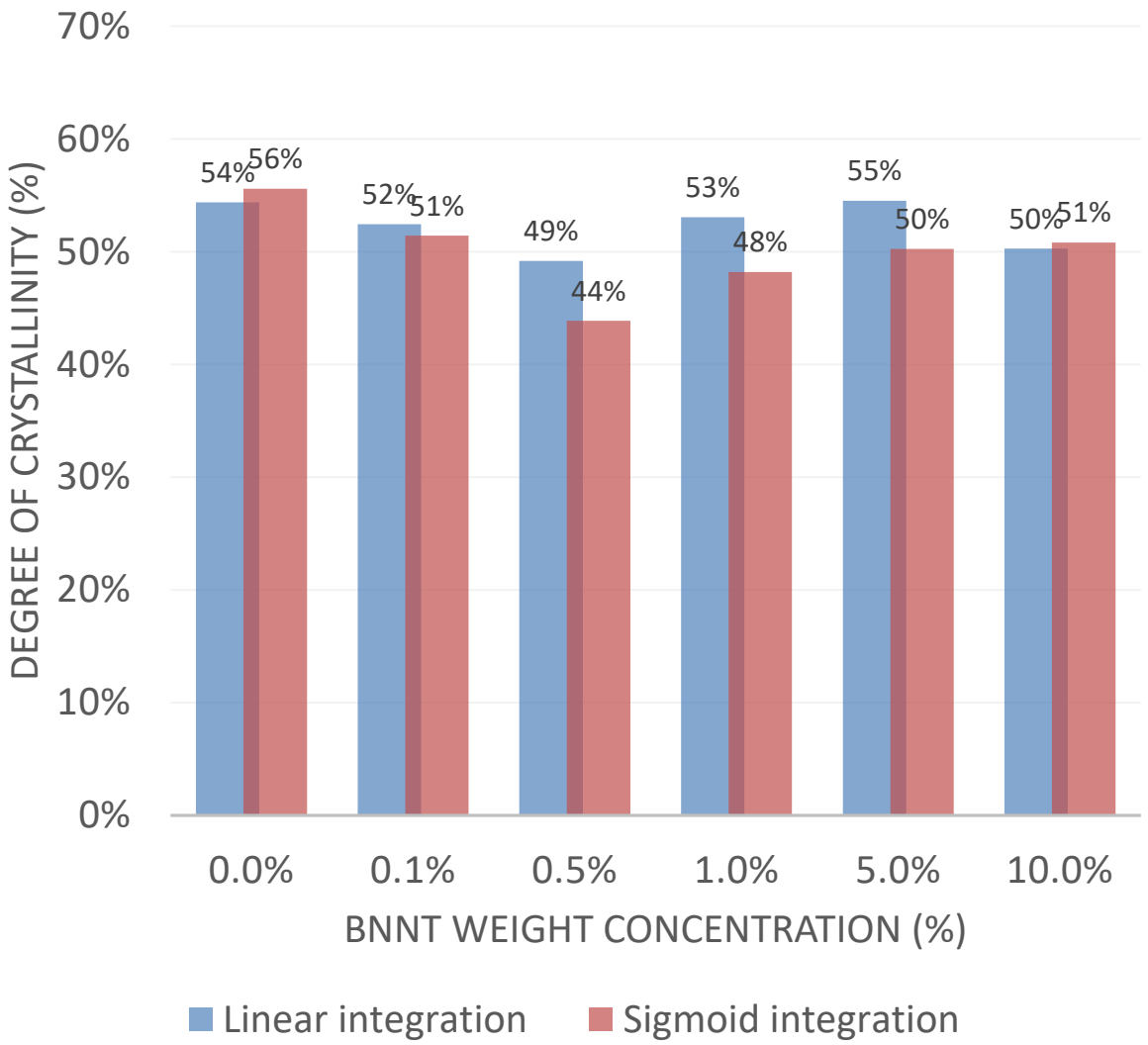

- Enthalpy integral range : 100 ℃ to 200 ℃
- BNNT fractions were compensated
- Linear / sigmoid integration

Degree of crystallinity (%)

$$X_C = \frac{\Delta H_f}{\Delta H_f^*} \times 100\%$$

Where ΔH_f^* is the melting enthalpy for a 100% crystalline PVDF, ΔH_f is the melting enthalpy of PVDF composite measured in DSC.

PVDF crystal patterns in XRD analysis

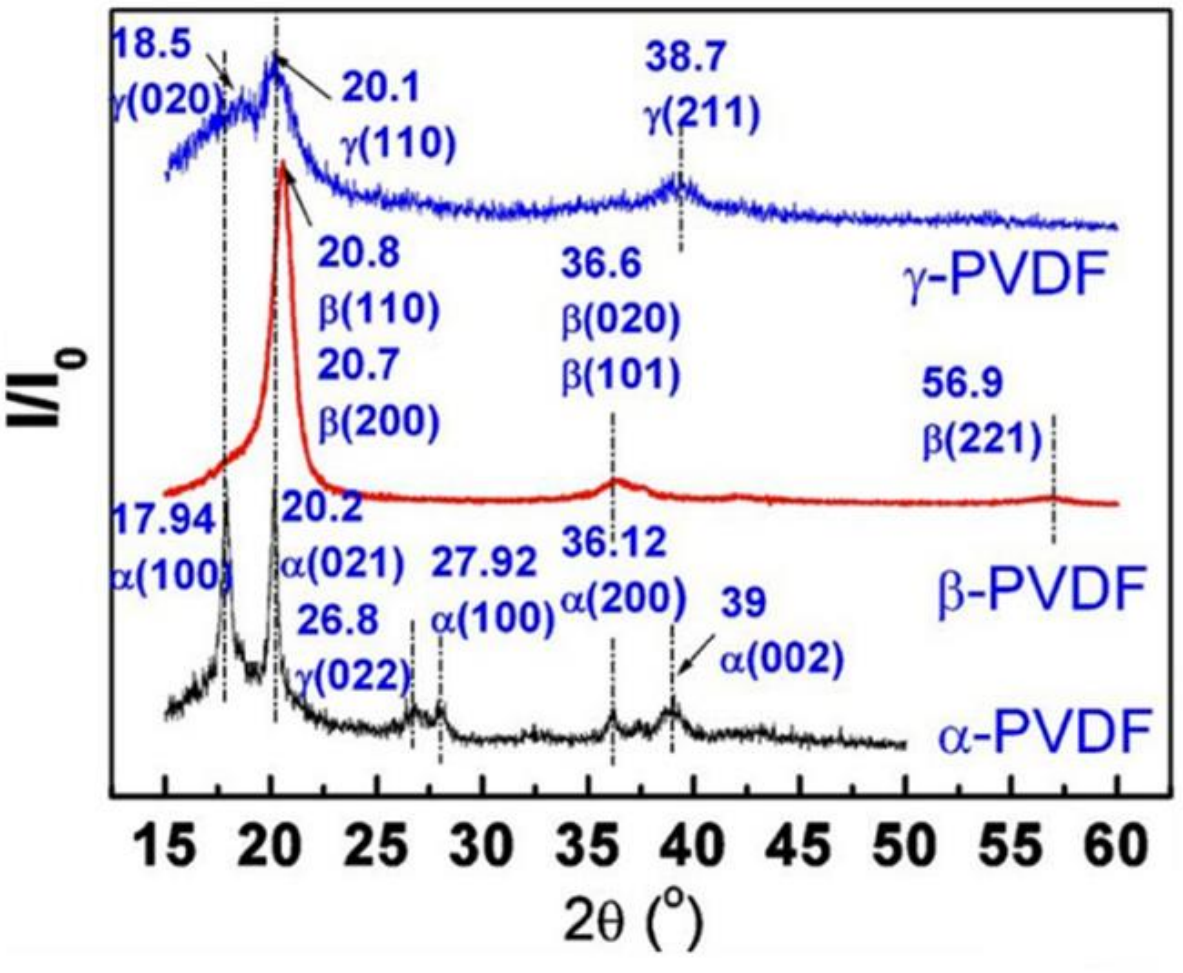

Typical XRD pattern of *α*, *β* and *γ*-PVDF and their crystal planes

Diffraction crystal plane and angle of different phase of PVDF

Crystal phase	2 θ	Crystal plane
α	17.9 18.5 20.2 27.9 36.1 39.0	(100) (020) (021) (111) (200) (002)
β	20.7 36.6 56.9	(110)(200) (020)(101) (221)
γ	18.5 20.2	(020) (110)

Kabir, Ekramul, et al., *Journal of Physics D: Applied Physics* (2017)

FTIR analysis of as precipitated BNNT-PVDF

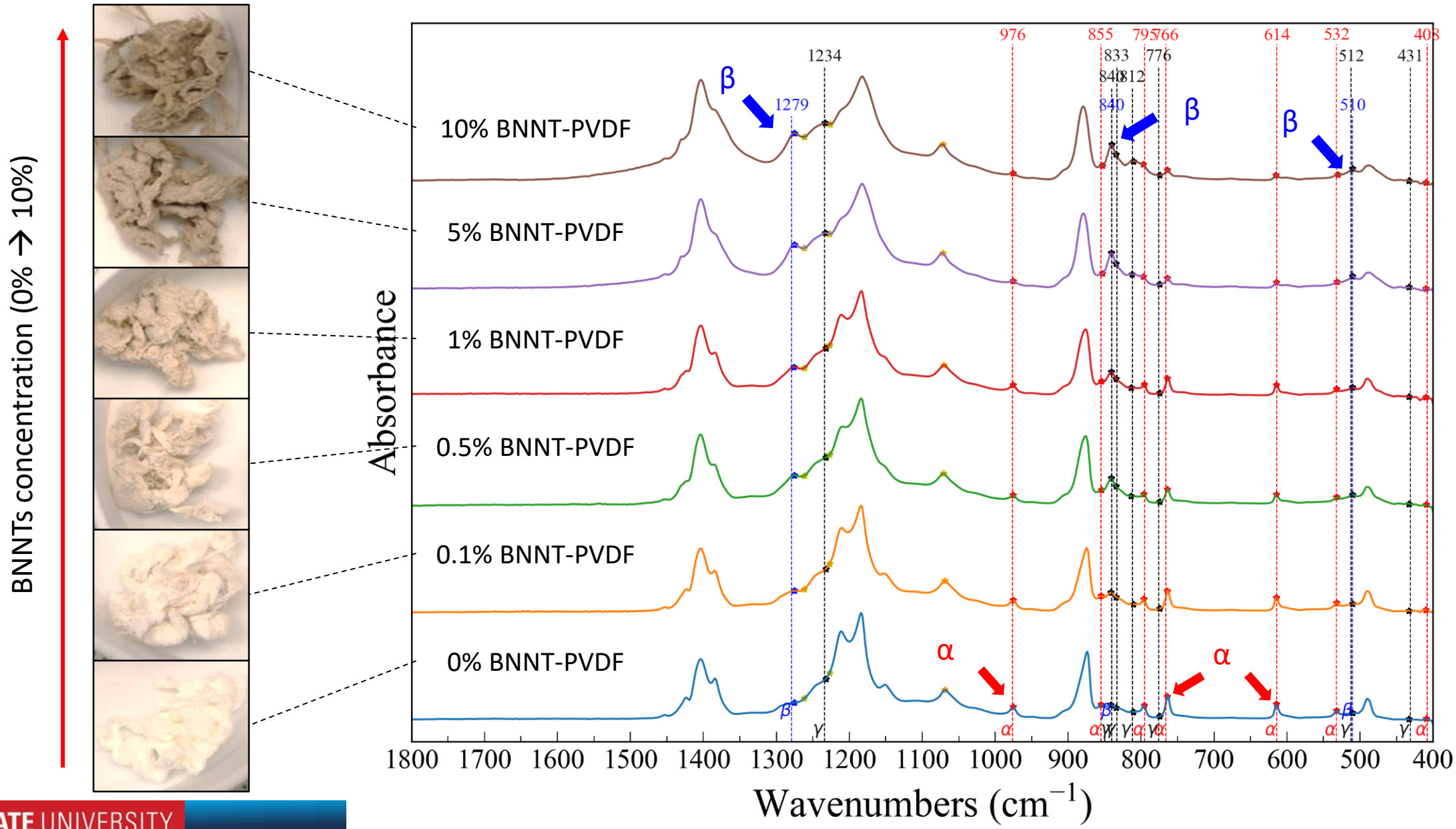

Polar fractions (%) of as precipitated BNNT-PVDF

NATIONAL INSTITUTE OF AEROSPACE

Peak-valley method

$$F(\beta) = \frac{A_\beta}{(K_\beta/K_\alpha)A_\alpha + A_\beta}$$

A_i: absorbance at I cm^{-1}
K_α: 6.1 x 10^4 cm^2mol^{-1}
K_β: 7.7 x 10^4 cm^2mol^{-1}

$$F(\beta) = F_{EA} \times \left(\frac{\Delta I_{\beta'}}{\Delta I_{\beta'} + \Delta I_{\gamma'}} \right)$$

$$F(\gamma) = F_{EA} \times \left(\frac{\Delta I_{\gamma'}}{\Delta I_{\beta'} + \Delta I_{\gamma'}} \right)$$

$\Delta I_{\beta'}$: intensity difference between 1275 & 1260 cm^{-1}
$\Delta I_{\gamma'}$: intensity difference between 1234 & 1225 cm^{-1}

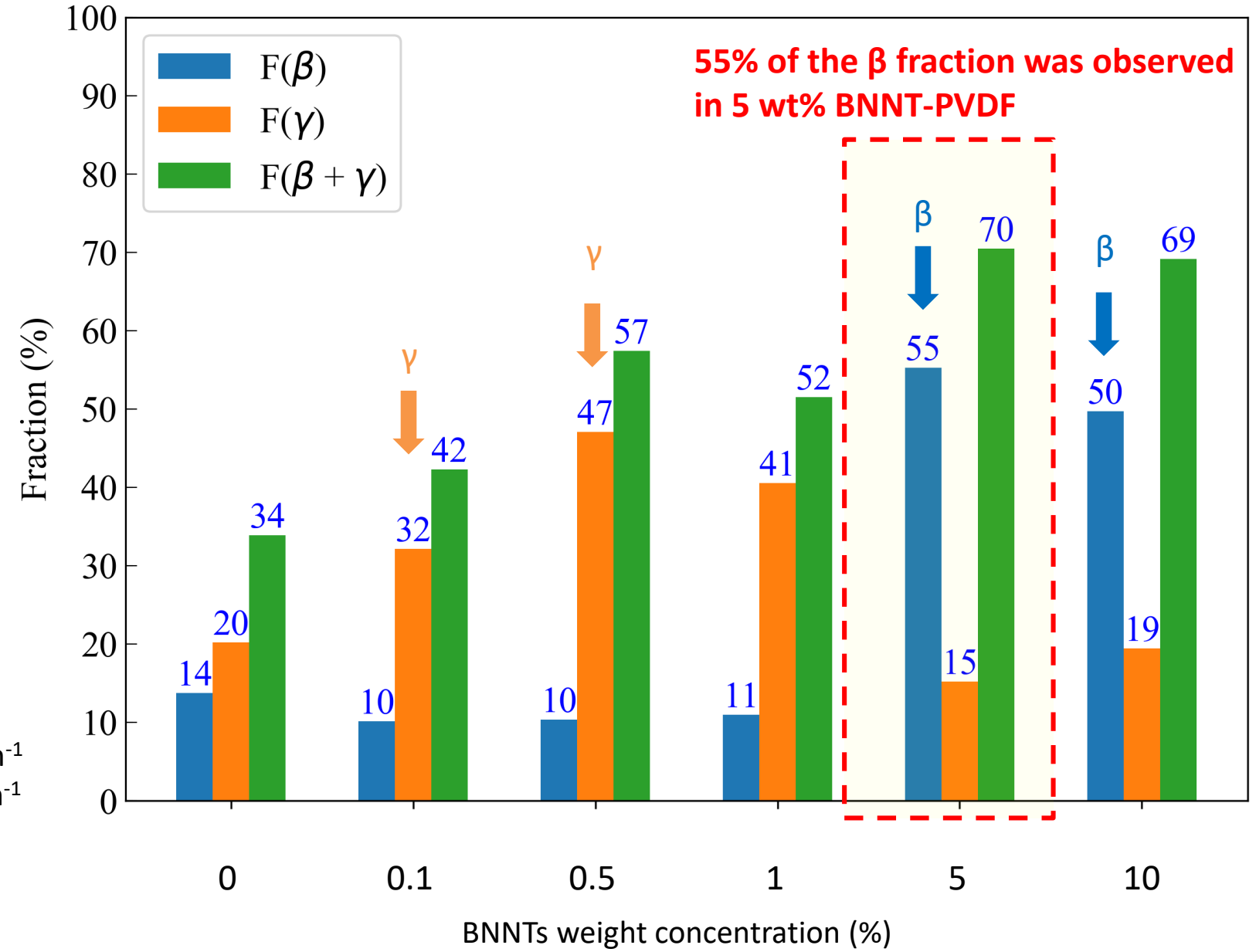

Shepelin, Nick A., et al., *Energy & Environmental Science* (2019)